JOURNAL OF THEORETICAL AND APPLIED MECHANICS
60, 4, pp. 673-685, Warsaw 2022
https://doi.org/10.15632/jtam-pl/156181

A CONTROL STRATEGY OF A PERMANENT MAGNET SYNCHRONOUS MOTOR FOR AN ELECTRIC VEHICLE

Jianxin Xie, Zimeng Liu

College of Intelligent Manufacturing, Qingdao Huanghai University, Qingdao, China

Corresponding author Jianxin Xie, e-mail: jasonxjx@126.com

The traditional modulation method of the inverter in a permanent magnet synchronous motor (PMSM) is lengthy and computationally intensive. Based on this, a simplified sinusoidal pulse width modulation method is proposed. In this method, voltage space vectors in each sector are synthesized, and the sector in which the synthesized vector is located is determined by the rotation angle of the resultant vector, and then the acting time of the basic vector is calculated by the voltage difference of the phase voltage. The problem of trigonometric functions and coordinate conversion is not involved in the whole calculation process, the calculation model is simple, and it is easy to realize digitization. Mathematical modeling is carried out by using the simulation software MATLAB, and the correctness of the calculation method after optimization is verified, which provides an idea for the later research of the inverter modulation method.

Keywords: PMSM, SVPWM method, argument, voltage difference

1. Introduction

With the development of new energy vehicle technology, the performance of electric vehicles continues to improve, battery and motor technology have made a great progress. PMSM (Permanent Magnet Synchronous Motor) has been widely used in electric vehicles. The inverter is a key component in PMSM. Its working efficiency directly affects energy loss of the motor and matching with other equipment (Fei and Shao, 2018; Hu *et al.*, 2021). Its working output efficiency depends on modulation method. In order to improve the control performance of PMSM and enhance its working stability in electric vehicles, experts at home and abroad have conducted necessary research on the control strategy of the PMSM inverter Blaschlk. A German motor expert proposed the an inverter vector control strategy and added relevant self-applicable, fuzzy and other control algorithms, which is a relatively advanced control method. There are two main modulation methods of PMSM inverter in China, one is sinusoidal pulse width modulation (SPWM) and the other is space vector pulse width modulation (SVPWM). SPWM is a modulation pulse mode. Its pulse width duty cycle outputs a sinusoidal waveform according to the sinusoidal law, which is used to control the on-off state of switching devices in the inverter circuit. It is a widely used inverter control mode, but it uses a coordinate system to calculate the trigonometric function, and the algorithm and control program are complex. The SVPWM method regards the inverter and the motor as a whole, and uses eight basic voltage vectors to synthesize the desired voltage vector to establish the switching state of the inverter power device. It uses the orthogonal coordinate system for calculation, which is simpler than the SPWM method. The SVPWM method can significantly reduce the harmonic of the inverter output current, reduce the power loss, and has high voltage utilization. It is widely used in PMSM. Because the calculation of the SVPWM method before optimization needs to repeatedly transform and adjust the orthogonal coordinate system, and involves complex calculation of the trigonometric

function, after the transformation of the orthogonal coordinate system, although the coordinate adjustment problem is solved, the calculation of the trigonometric function is still very complex. The SVPWM method without optimization is lengthy and has a large amount of calculation (Wang *et al.*, 2019; Zhao *et al.*, 2019). In this paper, the SVPWM calculation method in the PMSM inverter is optimized, the voltage space vector in each sector is synthesized. The sector is judged by the rotation angle of the synthesized vector, and then the action time of the basic vector is found. The optimized calculation model of the SVPWM method is simple and easy in realizing digitization (Deng *et al.*, 2018; Wu *et al.*, 2018; Luo *et al.*, 2019; Li *et al.*, 2018).

2. The basic mathematical model of a permanent magnet synchronous motor

A permanent magnet synchronous motor is usually divided into a surface mounted permanent magnet synchronous motor and an embedded permanent magnet synchronous motor. This paper mainly studies the surface mounted permanent magnet synchronous motor. Therefore, the permanent magnet synchronous motor mentioned later refers to the surface mounted permanent magnet synchronous motor. This paper is based on the permanent magnet synchronous motor. Therefore, we must first understand a mathematical model of the permanent magnet synchronous motor. Here, we first introduce the mathematical model of it. The stator of the permanent magnet synchronous motor has three-phase symmetrical windings of a, B and C, the rotor is equipped with permanent magnets, and the stator and rotor are coupled through air gap magnetic field. Due to the relative motion between the stator and rotor, the electromagnetic relationship is very complex. In order to simplify the analysis, the following assumptions are usually made:

- ignore the saturation effect of the iron core,
- ignore the winding leakage inductance of the motor,
- there is no damping winding on the rotor: the conductivity of permanent magnet material is 0,
- regardless of eddy current and hysteresis loss, the magnetic circuit is considered to be linear,
- the induced electromotive force of the stator phase winding is a sinusoidal wave, and the current of the stator winding only produces a sinusoidal magnetic force in the air gap, ignoring the high-order harmonic of the magnetic field (Zhao *et al.*, 2019; Ke *et al.*, 2019; Cheng *et al.*, 2019).

In the ABC coordinate system, the rotor of the permanent magnet synchronous motor is not symmetrical in the electrical and magnetic structure. The equation of the motor is a set of nonlinear time-varying equations related to the instantaneous position of the rotor, so the analysis of its dynamic characteristics is very difficult in the α-β system. In the 0 coordinate system, although the equation of the motor has been simplified after a linear transformation, the flux linkage and voltage equations of the motor are still a set of nonlinear equations. Therefore, the mathematical model of the motor in this coordinate system is generally not used in analysis and control. The vector control technology in the d-q-0 coordinate system solves this problem well, and changes the voltage and current into a direct flow, which simplifies the operation and analysis (Shanthi *et al.*, 2021; Petkar *et al.*, 2020; Sun *et al.*, 2019; Yu and Lu, 2019). In order to further understand the three coordinate systems, they are combined together, as shown in Fig. 1.

Through the above analysis, we can know that the d-q-0 coordinate system is mainly used in motor control. This paper studies the d-q mathematical model of the permanent magnet synchronous motor. Therefore, in the following we will focus on the analysis of the d-q-0 coordinate

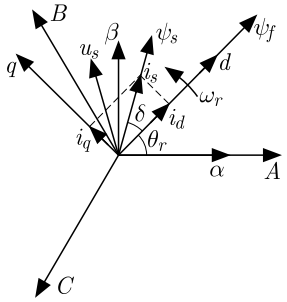

Fig. 1. Permanent magnet synchronous motor coordinate systems: A, B, C – stator three-phase static coordinate system, α, β – stator two-phase static coordinate system, d, q – rotor two-phase coordinate system, U_s – stator voltage, I_s – stator current, ψ_s – stator flux vector, ψ_f – rotor flux vector, θ_r – rotor angular position, δ – torque angle

system. It is a coordinate system that rotates synchronously with the stator magnetic field. The direction of F is consistent. The counterclockwise rotation direction of q axis is 90° ahead of the electrical angle of d axis, and the counterclockwise direction is taken as the positive direction of speed (Jin *et al.*, 2020; Krzysztofiak *et al.*, 2020; Zhang *et al.*, 2008).

The stator voltage equations in the DQ axis coordinate system are

$$u_d = \frac{d\psi_d}{dt} + R_s i_d - \omega_r \psi_q \qquad u_q = \frac{d\psi_q}{dt} + R_s i_q + \omega_r \psi_d \tag{2.1}$$

Their matrix form is

$$\begin{bmatrix} u_d \\ u_q \end{bmatrix} = \begin{bmatrix} R_s + pL_d & -w_e L_q \\ w_e L_d & R_s + pL_q \end{bmatrix} \begin{bmatrix} i_d \\ i_q \end{bmatrix} + \begin{bmatrix} 0 \\ w_e \psi_f \end{bmatrix} \tag{2.2}$$

The stator flux equations are

$$\psi_d = \psi_f + L_d i_d \qquad \psi_q = L_q i_q \tag{2.3}$$

The electromagnetic torque equation is

$$T_e = \frac{3}{2} p(\psi_d i_q - \psi_q i_d) = \frac{3}{2} p i_q [\psi_f + (L_d - L_q) i_d] = T_{e1} + T_{e2} \tag{2.4}$$

The first term is the electromagnetic torque generated by the interaction between the stator current and permanent magnet excitation magnetic field, which is called the permanent magnet torque. The second term is caused by the rotor salient effect, which is called the reluctance torque. Because the surface mounted permanent magnet synchronous motor is used here, and $L_d = L_q$, its electromagnetic torque equation can be expressed as

$$T_e = \frac{3}{2} p(\psi_d i_q - \psi_q i_d) = \frac{3}{2} p i_q \psi_f \tag{2.5}$$

The equation of motion is

$$J \frac{d\omega_m}{dt} = T_e - T_L - B\omega_m \tag{2.6}$$

The symbols denote: u_d, u_q – components of stator voltage, i_d, i_q – components of stator current, ψ_d, ψ_q – components of stator flux linkage, L_d, L_q – inductances of stator winding, ψ_f – flux linkage generated by the rotor permanent magnet, R_s – resistance of stator winding, T_e – electromagnetic torque, T_L – load torque, J – moment of inertia, p – polar logarithm, ω_r – electric angular velocity, ω_m – mechanical angular velocity, B – magnetic field intensity.

3. Implementation principle of SPWM

SPWM uses the output sinusoidal signal as the modulation wave and the high-frequency triangular wave as the carrier wave to control the on and off state of the upper and lower switches of one bridge arm of the inverter. If only the switch tube of the upper (lower) bridge arm is turned on and off repeatedly within a half of the sinusoidal cycle, and the switch tube of the lower (upper) bridge arm acts, it is called unipolar SPWM (Sun *et al.*, 2019). If the switching tubes of the upper and lower bridge arms are turned on and off alternately in the whole cycle, that is, the states of up on and down off and up off and down on are switched repeatedly, it is called bipolar SPWM. The schematic diagram of its implementation is shown in Fig. 2. It can be seen from the figure that when the carrier wave intersects with the modulation wave, the switching action time and switching on-off state of the bridge arm switching device of the inverter are determined by the intersection, and a series of positive and negative rectangular pulse voltage waveforms with different widths are obtained (Takahata *et al.*, 2019). The pulse sequence is characterized by an equal amplitude and unequal width, and its width changes according to the sinusoidal law. The theoretical basis of SPWM modulation is the principle of area equivalence, and the horizontal axis in Fig. 2 represents time. Therefore, the theoretical basis of SPWM is actually the principle of time average equivalence. When the number of pulses is enough, it can be considered that the fundamental amplitude and modulation amplitude of the inverter output voltage are equal (Wu *et al.*, 2019).

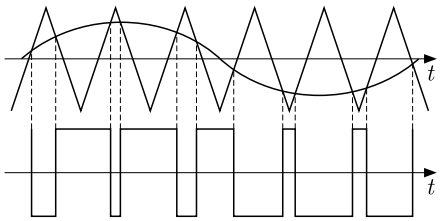

Fig. 2. Implementation of SPWM modulation

4. Simplification of the system model of PMSM

First of all, the three-phase stationary coordinate system of the three-phase current in the PMSM should be transformed into a two-phase stationary coordinate system by a CLARK change. It is then transformed into a two-phase rotating coordinate system by performing a PARK change. In this way, the sector can be judged by the rotated argument, and the mathematical model of the PMSM can be greatly simplified, as shown in Fig. 3.

The excitation component and torque component generated by the current flowing through the stator in PMSM are decoupled by two transformations. The PMSM control unit adopts the sensor signal feedback mode for double closed-loop control. In the control process, $i_d = 0$ is used to control the stator current vector to be located in the coordinate axis without other components, so that all the current is used to generate the torque. A PI controller and PLL phase--locked loop lock locate the stator current. After the reverse Park transform ($Park^{-1}$), v_α^*, v_β^* are obtained, and then the SVPWM control strategy algorithm is optimized and the inverter is controlled.

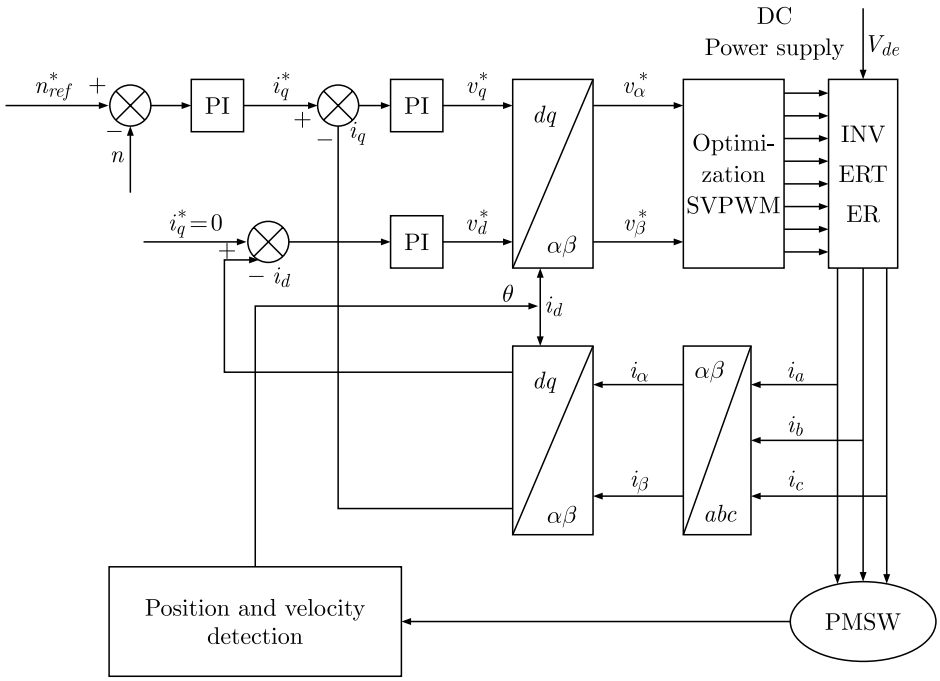

Fig. 3. Diagram of the simplified PMSM electronic control unit

5. Optimization of SVPWM algorithm

5.1. Traditional SVPWM algorithm

The traditional SVPWM still uses the space vector method to calculate the voltage value. As shown in Fig. 4, six voltages from U1 to U6 are calculated by the space vector method. Since only U3 and U4 are in the coordinate axis α, the calculation is more convenient. The remaining four voltages are distributed in the vector space and cannot be directly represented by the α-β coordinate axis. They need to go through trigonometric operations, and the algorithm is complicated.

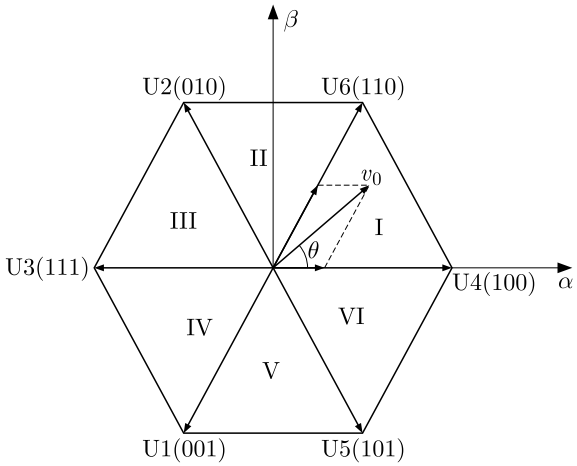

Fig. 4. Voltage vector space distribution

5.2. Optimization of the traditional SVPWM algorithm

First, as shown in Fig. 1, v_α^*, v_β^* are transformed by $Park^{-1}$ transform

$$\begin{bmatrix} v_a \\ v_b \\ v_c \end{bmatrix} = \frac{2}{3} \begin{bmatrix} 1 & 2 & \frac{1}{\sqrt{2}} \\ -\frac{1}{2} & \frac{3}{\sqrt{2}} & \frac{1}{\sqrt{2}} \\ -\frac{1}{\sqrt{2}} & -\frac{3}{\sqrt{2}} & \frac{1}{\sqrt{2}} \end{bmatrix} \begin{bmatrix} v_\alpha^* \\ v_\beta^* \\ 0 \end{bmatrix} \tag{5.1}$$

where three-phase voltage v_a, v_b, v_c is obtained through $Park^{-1}$ transform, which is converted into three-phase sinusoidal voltage

$$v_a = V_m \cos\theta \qquad v_b = V_m \cos\Big(\theta - \frac{2\pi}{3}\Big) \qquad v_c = V_m \cos\Big(\theta + \frac{2\pi}{3}\Big) \tag{5.2}$$

Among them, V_m is the highest value of the three-phase voltage.

Synthesize the v_a, v_b, v_c three-phase voltages into * (space voltage vector), whose expression is

$$v_{ref} = v_a + v_b \exp\Big(\mathrm{j}\frac{2\pi}{3}\Big) + v_c \exp\Big(-\mathrm{j}\frac{2\pi}{3}\Big) = \frac{3}{2} V_m \exp(\mathrm{j}\omega t) \tag{5.3}$$

Then use the Euler formula to calculate $V_m \exp(\mathrm{j}\omega t)$ in (5.3)

$$V_m \exp(\mathrm{j}\omega t) = V_m(\cos\omega t + \mathrm{j}\sin\omega t) \tag{5.4}$$

where v_{ref} is the voltage vector obtained by rotating counterclockwise in space according to a certain angular frequency ω. According to the geometric meaning of the complex number, its amplitude remains unchanged, its absolute value is $3V_m/2$, and its amplitude $\theta = \omega t$, indicating that θ changes according to the angular frequency ω. Bring the value into Eqs. (5.3) and (5.4) and input it to the simulation module. The waveform of output θ is shown in Fig. 5.

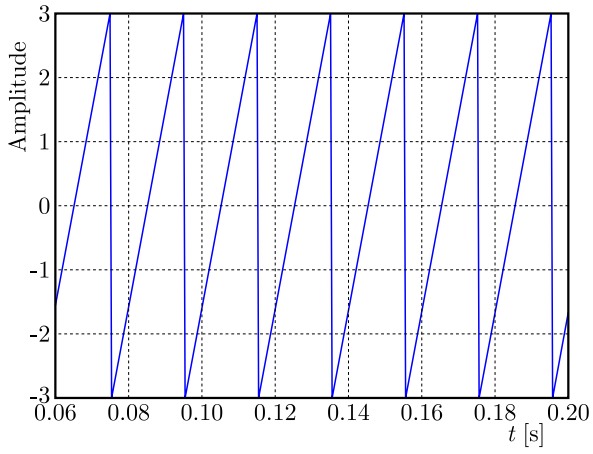

Fig. 5. Angle θ output waveform

Through the analysis of Fig. 5, it can be seen that the amplitude of v_{ref} changes with a change of the argument angle θ, and the amplitude represents the position of v_{ref}. Generally, the argument angle is taken between $[-\pi, \pi]$ and the sector calculation of the space vector is carried out in the way of $3\theta/\pi$ rounding. The sector is defined as H, and its expression is

$$H = \frac{3\theta}{\pi} + 3 \tag{5.5}$$

Determine the corresponding relationship between H and sectors according to Eq. (5.5). Assuming v_{ref} is in a sector, $\theta = \pi/4$, bring it into Eq. (5.5), and round up the calculated value to obtain $H = 4$. The corresponding relationship between the value of H and the sector is obtained in turn, as shown in Table 1.

Table 1. Sector, H correspondence table

Sector	IV IV	V V	VI VI	I I	II II	III III
H	1	2	3	4	5	6

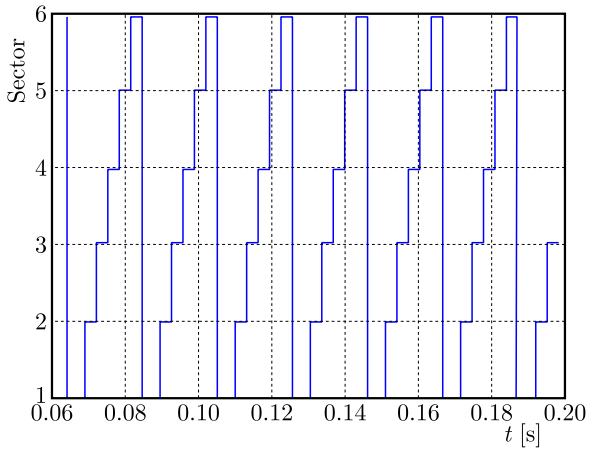

Fig. 6. Sector simulation waveform

According to Fig. 4, assuming v_{ref} is still at the position of the first sector, analyze the action time of the voltage vector, which can be calculated by the principle of the volt-second balance

$$v_{ref}T_s = U_4T_x + U_6T_y \tag{5.6}$$

Among them: T_x, T_y is the action time of the basic voltage vector, T_s – action cycle.

According to the sine principle

$$\frac{U_B}{\sin\left(\frac{\pi}{3} - \theta\right)} = \frac{U_A}{\sin\theta} = \frac{|v_{ref}|}{\sin\frac{2\pi}{3}} \tag{5.7}$$

Among them, $U_A = |U_6|T_y/T_s$, $U_B = |U_4|T_x/T_s$ are calculated

$$T_x = mT_s\sin\left(\frac{\pi}{3} - \theta\right) \qquad T_y = mT_s\sin\theta \tag{5.8}$$

and $|U_6| = |U_4| = V_{dc}$, the modulation ratio $m = 2|v_{ref}|/V_{dc}\sqrt{3}$.

Expand (5.8) to calculate

$$T_x = \frac{|v_{ref}|T_s\left(\cos\theta - \frac{1}{\sqrt{3}}\sin\theta\right)}{V_{dc}} \qquad T_y = \frac{|v_{ref}|T_s\sin\theta}{V_{dc}} \tag{5.9}$$

v_a minus v_b to obtain

$$v_a - v_b = |v_{ref}|\left(\cos\theta - \frac{1}{\sqrt{3}}\sin\theta\right) \tag{5.10}$$

Among them $|v_{ref}| = 3V_m/2$. From equation (5.10)

$$\cos\theta - \frac{1}{\sqrt{3}}\sin\theta = \frac{1}{v_{ref}}(v_a - v_b) \tag{5.11}$$

v_b minus v_c to obtain

$$v_b - v_c = \frac{2}{\sqrt{3}}|v_{ref}|\sin\theta \tag{5.12}$$

Expand (5.12) to calculate

$$\sin\theta = \frac{\sqrt{3}}{2|v_{ref}|}(v_b - v_c) \tag{5.13}$$

Substituting formulas (5.11) and (5.13) into (5.9), one gets

$$T_x = \frac{T_s(v_a - v_b)}{V_{dc}} \qquad T_y = \frac{T_s(v_b - v_c)}{V_{dc}} \tag{5.14}$$

Through derivation of the above formula, it can be known that the magnitude relationship of the three-phase voltage is $v_a > v_b > v_c$. From formula (5.14), it can be known that the basic voltage vector action time of T_x, T_y is only related to the difference of the three-phase voltage, and has nothing to do with other factors. Moreover, the basic voltage vector action time of T_x, T_y only needs to perform addition and subtraction operations and does not need to perform trigonometric operations. The overall calculation amount is reduced, and the calculation method is greatly simplified.

No matter which sector position v_{ref} is in, its action time is only related to the three-phase voltage difference. According to the above analysis, the acting time of the three upper bridge arms in one action period are

$$\begin{aligned} T_{aon} &= \frac{T_s - T_x - T_y}{4} \qquad T_{bon} = \frac{T_s - T_x - T_y}{4} + \frac{T_x}{2} \\ T_{con} &= \frac{T_s - T_x - T_y}{4} + \frac{T_x}{2} + \frac{T_y}{2} \end{aligned} \tag{5.15}$$

According to formula (5.15), the action time of the three bridge arms of any sector can be calculated.

6. Simulation verification

Firstly, the mathematical modeling is carried out by using the simulation software MATLAB. Set the parameters of PMSM, as shown in Table 2.

Table 2. PMSM parameter setting of the synchronous motor

Stator winding resistance [Ω]	Stator d-axis inductance [H]	Stator q-axis inductance [H]	Motor moment of inertia [kgm^2]	Number of poles
3.105	0.0075	0.0085	0.0002	4

Set the parameters of the voltage regulator and current regulator in PMSM, $K_p = 0.392$, $K_1 = 16.01$, $K_p = 1.45$, $K_1 = 120.1$. Input the above parameters into the simulation software until the PMSM runs stably, and the output stator current waveform is shown in Fig. 7.

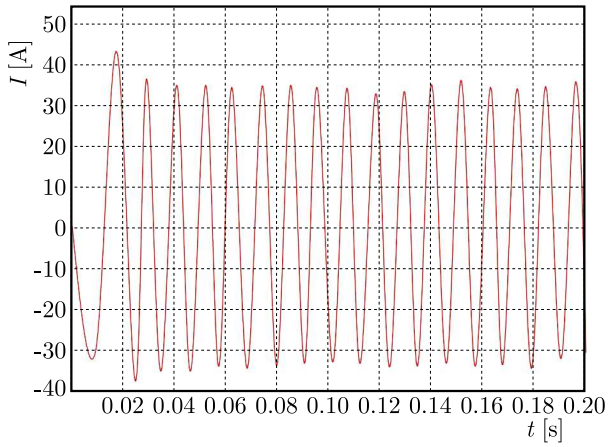

Fig. 7. Stator current waveform

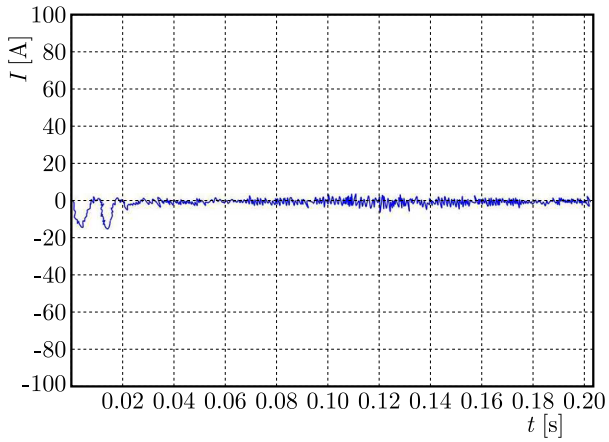

Fig. 8. Stator d-axis current waveform

The current of the axis d is simulated, and the output waveform is shown in Fig. 8. According to the analysis of the output waveform, the current of PMSM is unstable and fluctuates slightly at the initial stage of operation. After the operation is stable, the current of the axis d is basically zero, which is consistent with the i_d^* value set in the theoretical analysis.

Set the operating torque of PMSM to 5 Nm. Through the analysis of Fig. 9, after the PMSM operates stably, the torque waveform changes little and is relatively stable.

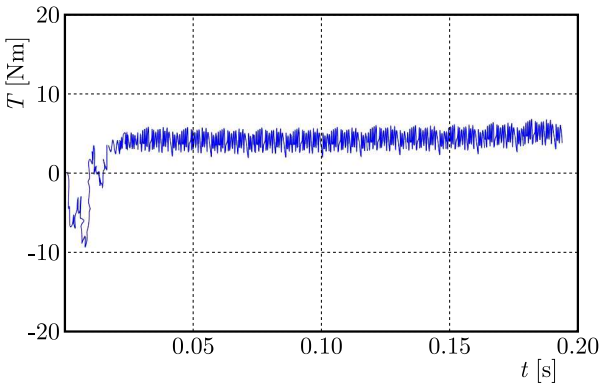

Fig. 9. PMSM torque waveform

Set the operating speed of PMSM to 750 r/min. Through the analysis of Fig. 10, after the PMSM operates stably, the speed waveform changes slightly and is relatively stable.

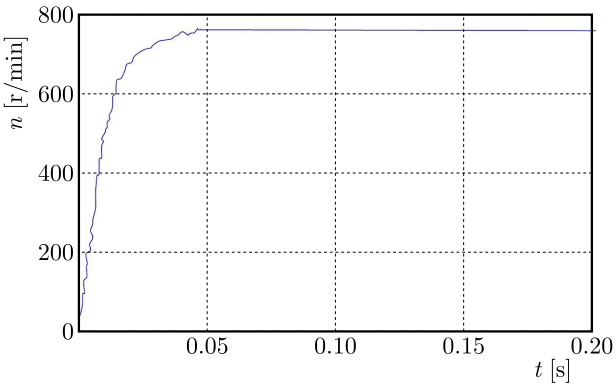

Fig. 10. PMSM speed waveform

The optimized SVPWM algorithm is input into the simulation software to control PMSM. The simulation results can be analyzed from Fig. 7 to Fig. 10. PMSM operates stably and has a fast dynamic response. The optimized SVPWM algorithm is correct and applicable.

7. Experimental verification

The accuracy of the simulation results needs to be verified by experiments, and the PMSM control experimental platform is built. The experimental platform mainly includes the permanent magnet synchronous motor, oscilloscope, multimeter, drive circuit board, control circuit board, PC, etc. for testing, as shown in Fig. 11. Among them, the input parameters of the permanent magnet synchronous motor in the test have been given in "3 simulation verification".

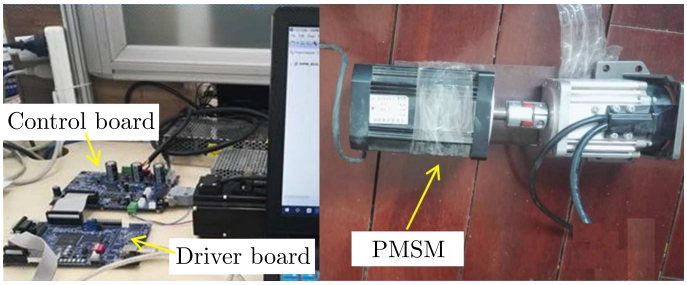

Fig. 11. PMSM test bench

The operating torque of the PMSM is set to 5Nm, and the output operating torque curve is shown in Fig. 12. After the PMSM runs stably, the output torque waveform is stable, and the waveforms are basically consistent with the simulation results.

Set the operating speed of PMSM to 3000 r/min, and the output operating speed curve is shown in Fig. 13. After the PMSM operates stably, the speed waveform is relatively stable, which is basically consistent with the simulation results.

Therefore, it can be determined that the simulation results are consistent with the experimental results. The optimized SVPWM algorithm is correct and applicable, which can ensure the stable operation and fast dynamic response of PMSM.

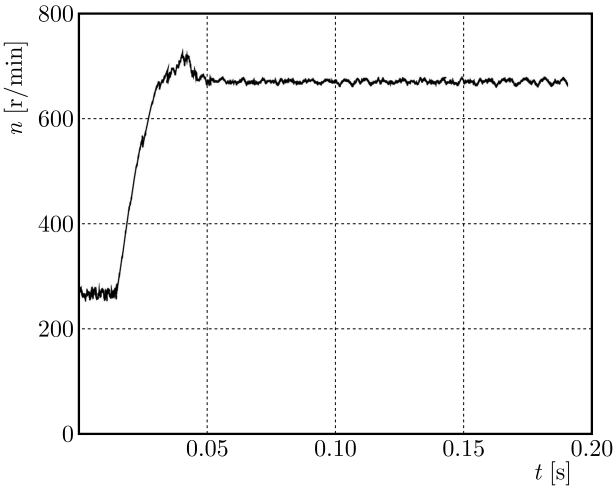

Fig. 12. PMSM output torque waveform

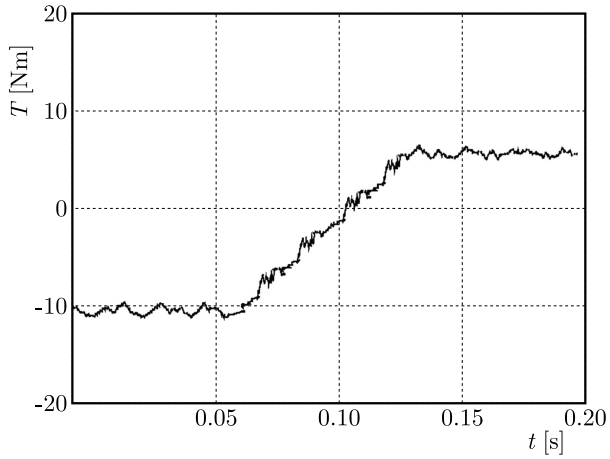

Fig. 13. Output speed waveform of PMSM

8. Conclusion

PMSM is more and more widely used in electric vehicles, but the modulation method of its inverter is difficult to realize because of complex factors such as synthetic vector rotation angle and period. In this paper, SVPWM method is adopted, and its calculation method is optimized. The sector where the vector is located is judged by the amplitude of the synthetic vector rotation, and then the action time of the basic vector is calculated. The calculation model is simple and easy to digitize. The mathematical modeling is carried out by using the simulation software MATLAB to verify the correctness of the optimized calculation method, and the working performance of the optimized PMSM is tested by building an experimental platform. The optimized permanent magnet synchronous motor can well meet the requirements of low-speed high torque, climbing high torque and high-speed stability of electric vehicles.

References

1. Cheng S.Q., et al., 2019, Research and implementation of vector control strategy for permanent magnet synchronous motor (in Chinese), *Journal of Hubei Institute of Automotive Industry*, **33**, 2, 55-59

2. Deng G.F., Wang H., Wu X., Huang S.D., Huang K.Y., 2018, A position sensorless control strategy for permanent magnet synchronous motor that can suppress the nonlinear influence of the inverter (in Chinese), *Chinese Journal of Electrical Engineering*, **38**, 24, 7381-7390+7464

3. Fei W.J., Shao D.G., 2018, Influence of PWM modulation on control performance of brushless DC motor (in Chinese), *Micromotor*, **51**, 8, 55-60

4. Hu C.M., Liu M.N., Wei C.Q., Wang T., 2021, Development of a collaborative controller for a dual-motor independent drive electric tractor (in Chinese), *Journal of Henan University of Science and Technology (Natural Science Edition)*, **42**, 1, 27-33+39+3-4

5. Jin F.Z., Wan H., Huang Z.F., Gu M.X., 2020, PMSM vector control based on fuzzy PID controller, *Journal of Physics: Conference Series*, **1617**, 1

6. Ke X.B., Guo L., Yuan X.F., Li Y., Xu X.L., 2019, Control of permanent magnet synchronous motor based on fuzzy sliding mode control strategy, *Machinery and Electronics*, **37**, 8, 60-63+68

7. Krzysztofiak M., Skowron M., Orlowska-Kowalska T., 2020, Analysis of the impact of stator inter-turn short circuits on PMSM drive with scalar and vector control, *Energies*, **14**, 1, 153

8. Li Y.B., Yang Z.X., 2018, Design and analysis of non-uniform magnetic pole disk type ironless permanent magnet ISG motor (in Chinese), *Journal of Henan University of Science and Technology (Natural Science Edition)*, **39**, 4, 28-33+6

9. Luo Y., Wu F., Liu Z.Y., Liu L., Qi P.W., Wei Y.H., 2019, Research on control strategy of permanent magnet synchronous motor for pure electric vehicle (in Chinese), *Journal of Chongqing University of Technology (Natural Science)*, **33**, 2, 1-7

10. Petkar S.G., Eshwar K., Thippiripati V.K., 2020, A modified model predictive current control of permanent magnet synchronous motor drive, *IEEE Transactions on Industrial Electronics*, **68**, 2, 1025-1034

11. Shanthi R., Kalyani S., Devie P.M., 2021, Design and performance analysis of adaptive neuro-fuzzy controller for speed control of permanent magnet synchronous motor drive, *Soft Computing*, **25**, 2, 1519-1533

12. Sun C.C., Gong G.F., Yang H.Y., Wang F., 2019, Fuzzy sliding mode control for synchronization of multiple induction motors drive, *Transactions of the Institute of Measurement and Control*, **41**, 11, 3223-3234

13. Sun X.L., Li Z.G., Wang X.L., Li C.J., 2019, Technology development of electric vehicles: A review, *Energies*, **13**, 1, 90

14. Takahata R., Wakui S., Miyata K., Noma K., Senoo M., 2019, Influence of rotor eccentricity on vibration characteristics of permanent magnet synchronous motor, *IEE Journal of Industry Applications*, **8**, 3, 558-565

15. Wang S.W., Wang W., Fan J.L., Tian X., 2019, Analysis and optimization of electromagnetic noise of permanent magnet synchronous motor for vehicles (in Chinese), *Automotive Technology*, **8**, 12-15

16. Wu Q.M., Wang T.T., Li X.Y., 2018, Efficiency optimization control of IPMSM for electric vehicles based on Mann iteration (in Chinese), *Micromotor*, **51**, 3, 11-17+42

17. Wu X., Xu Y.H., Liu J., Lv C., Zhou J.Z., Zhang Q., 2019, Characteristics analysis and fuzzy fractional-order pid parameter optimization for primary frequency modulation of a pumped storage unit based on a multi-objective gravitational search algorithm, *Energies*, **13**, 1, 137

18. Yu H.C., Lu C.G., 2014, Recent development of electric vehicles, *Applied Mechanics and Materials*, **490-491**, 968-971

19. Zhang C.M., Liu H.P., Chen S.J., Wang F.J., 2008, Application of neural networks for permanent magnet synchronous motor direct torque control, *Journal of Systems Engineering and Electronics*, **3**, 555-561

20. Zhao J.G., Zhang Q.H., Li H.J., 2019, Design and research based on an electric vehicle in-wheel motor structure (in Chinese), *Micromotor*, **52**, 9, 25-28

21. Zhao R.D., Zhao B., Xu H.L., Sun P.X., Dong X.M., 2019, Research on control system and strategy of permanent magnet synchronous motor with LC filter, *Journal of Electrotechnical Technology*, **34**, S1, 79-86

Manuscript received April 27, 2022; accepted for print September 19, 2022